Observation of Single Vortices Condensed into a Vortex-Glass Phase by Magnetic Force Microscopy

A. Moser, H. J. Hug, I. Parashikov, B. Stiefel, O. Fritz, H. Thomas, A. Baratoff, and H.-J. Güntherodt
Institut für Physik, Universität Basel, Klingelbergstrasse 82, CH-4056 Basel, Switzerland

P. Chaudhari
IBM Watson Research Center, Yorktown Heights, New York
(Received 21 April 1994)

A low temperature magnetic force microscope has been applied to spatially resolve single vortices in an epitaxially grown $YBa_2Cu_3O_{7-\delta}$ thin film at 77 K. A disordered vortex arrangement is observed, and the vortices are strongly pinned. The observed phase is expected to be truly superconducting due to strong pinning.

PACS numbers: 74.60.Ge, 61.16.Ch, 74.76.Bz

The first successful Bitter pattern experiment on a high-T_c superconductor (HTSC) showed a hexagonal vortex lattice at 4 K with the vortices carrying one flux quantum, $\phi_0 = 2.07 \times 10^{-15}$ Wb [1]. Since then measurements based on high-Q mechanical oscillators [2,3], I-V characteristics [4], SQUID picovoltametry [5], magnetization [6], and neutron diffraction [7] have shown a distinct boundary in the magnetic phase diagram of the vortex state, the so-called irreversibility line. It is now widely believed that above this line the vortex lattice undergoes a melting transition. Recent theoretical work combines this idea with quantum fluctuations of the vortices [8] to obtain an excellent agreement with experiments on $YBa_2Cu_3O_{7-\delta}$ (YBCO) single crystals. These experiments suggest the existence of a spatially fixed arrangement of vortices in YBCO single crystals and epitaxial thin films up to a few ten mT and up to temperatures close to T_c. Bitter pattern experiments failed to observe fixed vortex arrangements at 77 K, however.

The scanning tunneling microscope (STM) was used to image the vortex lattice of a $NbSe_2$ single crystal [9]. Since then additional experiments have been performed on $NbSe_2$ [10–13] or related materials [14]. However, STM experiments on HTSC often are not reproducible and can be very misleading. Although good tunneling spectra have been obtained [15], single vortices have not yet been detected by STM. Several authors, including ourselves, have pointed out [10–13] that the complex structure of HTSC materials and their surfaces, their short coherence lengths, and the high mobility of vortices even at low temperatures conspire to make a detection in HTSC of vortices rather difficult with the STM.

In contrast, the detection of a vortex via its magnetic stray field seems feasible since the penetration depth and thus the magnetic diameter of the vortices is large. Indeed, not only the Bitter technique, but also Lorentz microscopy [19] and scanning Hall probe microscopy [20] have successfully imaged single vortices. In a previous attempt [21], only vortex bundles could be imaged using a tunneling stabilized magnetic force microscope.

In this Letter we demonstrate for the first time that low temperature magnetic force microscopy is able to image single vortices in a YBCO thin film at 77 K. Our magnetic force microscope (MFM) does not require any special sample preparation and is able to image the same sample area under different conditions (temperature, magnetic field) repeatedly.

Our MFM has been described in detail elsewhere [22,23]. In contrast to other groups [24], we use a static operation mode, the variable deflection mode. This mode enables fast scanning and allows a precise spatial correlation of the magnetic stray field map with the topography. We usually obtain a (magnetic) force resolution below 10^{-12} N and a lateral resolution below 100 nm. Further, we have demonstrated the successful application of our instrument to study a HTSC [25,26] by detecting a different deflection of the cantilever upon approach either a zero-field cooled or a field-cooled sample.

In the experiment described here, we use a microfabricated cantilever made sensitive to magnetic stray fields by a 25 nm thick iron coating. The sensitivity and resolution has been tested on a magneto-optical disk at room temperature. Our sample is an epitaxial YBCO film of about 300 nm thickness grown onto a $SrTiO_3(001)$ substrate by laser ablation. A topographical image acquired at 77 K in the contact mode shows small hills with a diameter around 50 nm and a height of a few nanometers [Fig. 1(a)].

We perform the following steps to obtain the magnetic field map at different applied magnetic fields: First the tip is retracted from the sample to a separation of 2 mm and the sample is cooled in the external field. Then we approach the tip to the measurement position, i.e., to a tip-to-sample separation of about 20 nm. The magnetic field map in Fig. 1(b) shows two features corresponding to an attractive force of about 0.6×10^{-12} N. The observed deviation from a circular shape originates from the relatively low signal-to-noise ratio of 3:1. In order to prove that single vortices are imaged, we heat the sample above T_c to approximately 100 K, and cool it

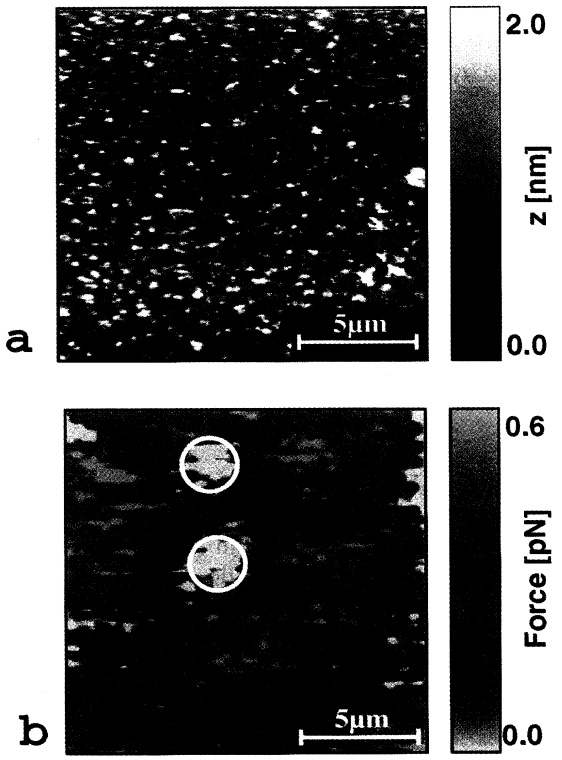

FIG. 1. (a) The surface of the epitaxially grown YBCO films is extremely smooth. The small hills have a diameter of about 50 nm and a height of only a few nanometers. These hills are believed to be screw dislocations. The step structure cannot be resolved, since the radius of the tip is expected to be around 30 nm. This topographical image is acquired with the tip in contact with the surface of the sample. (b) The same area is imaged with the tip not in contact with the sample. The two, circular features produce an attractive force of only 6×10^{-13} N. These features are images of single vortices. The sample was cooled in a field of 0.013 mT.

in various fields (Fig. 2). We observe seven features if we apply a field of 0.093 mT [Fig. 2(a)] and 15 in the case of 0.174 mT [Fig. 2(b)]. These features generate an attractive force since the applied field is parallel to the direction of the magnetization of the MFM tip. If the external field is *reversed,* its direction is antiparallel to the magnetization of the tip, and we expect each feature to produce a repulsive force. Indeed we observe two inversed features if we apply a field of -0.068 mT [Fig. 2(c)] and 14 in the case of -0.149 mT [Fig. 2(d)]. The number of these features scales linearly with the applied field while the attraction and repulsion of the tip to these features depend on the direction of the applied field (Fig. 3). A fit to the data gives a flux of $(1.93 \pm 0.12) \times 10^{-15}$ Wb per feature. We conclude that these features are images of single vortices carrying one single flux quantum of 2.07×10^{-15} Wb.

If all vortex positions shown in Figs. 1(b) and 2(a)–2(d) are arranged in one graph (Fig. 4), we find the vortices to be pinned to many different positions. Thus the two vortices imaged in Fig. 1(b) could be pinned to any of the other positions. Indeed, we observe two vortices pinned to different positions in Fig. 2(d) for a field of similar size but opposite direction. Furthermore, the observed arrangements of vortices are stable on a time scale of several hours. We conclude that the tip does not drag any vortices. Otherwise, they would have become pinned to one of the many pinning centers sooner or later. From these observations we conclude that the vortices are generated by the externally applied field and certainly not by the stray field of the MFM tip, and that we observe all vortices, i.e., no vortices are nucleated or moved around by the scanning tip. The stray field of the tip is prevented from penetrating into the superconductor by screening currents; thus the HTSC is not in the thermodynamical equilibrium state when the tip is approached to the working distance (~20 nm).

The force above a vortex is below 10^{-12} N, which is much smaller than expected from calculations [17,27]. At first glance it seems astonishing that the force is that low and that vortices can nevertheless be imaged, since even thin film tips are expected to produce fields larger than the first critical field at our working distance [28]. The microscopic structure of the magnetization, assumed constant in model calculations of stray fields of magnetic tips [28], might be much more complex in reality.

In our images we observe disordered vortex arrangements. In Fig. 2(b) the smallest intervortex distance (around 2 μm) differs strongly from the expected value for a triangular vortex lattice (5 μm). The vortex arrangement is dominated by pinning rather than by the elastic intervortex energies. Fisher and co-workers [29] have shown that in a two-dimensional system with pointlike pins the vortex lines should freeze into a vortex-glass phase, and conjectured that a similar phase occurs below the irreversibility line in real HTSC. This vortex-glass phase is predicted to be a true superconductor with $R = 0$. Koch *et al.* [4] found a transition at a well-defined temperature from a resistive state into a superconducting state upon cooling in strong magnetic fields in a laser-ablated YBCO thin film. Later, Nelson and Vinokur [30] discussed pinning by spatially correlated disorder and pointed out that the experiment of Koch *et al.* may well be affected by defects extending through the film, like twin planes, edge, or screw dislocations. The typical morphology of the laser-ablated film, as well as measurements of the disordered vortex arrangements following successive thermal cycles, suggest indeed that the vortices are condensed into a vortex-glass phase. However, further studies concerning the nature of the pinning centers and measurements in higher fields are needed to confirm this hypothesis. Note that the vortices do not move, although the tip generates a lateral force acting on the vortices. According to our model calculations [17], the lateral force exerted by the tip on a single vortex is about a factor of four smaller than the vertical force. With a measured vertical force around 6×10^{-13} N, we expect a lateral force in the low 10^{-13} N range. Since

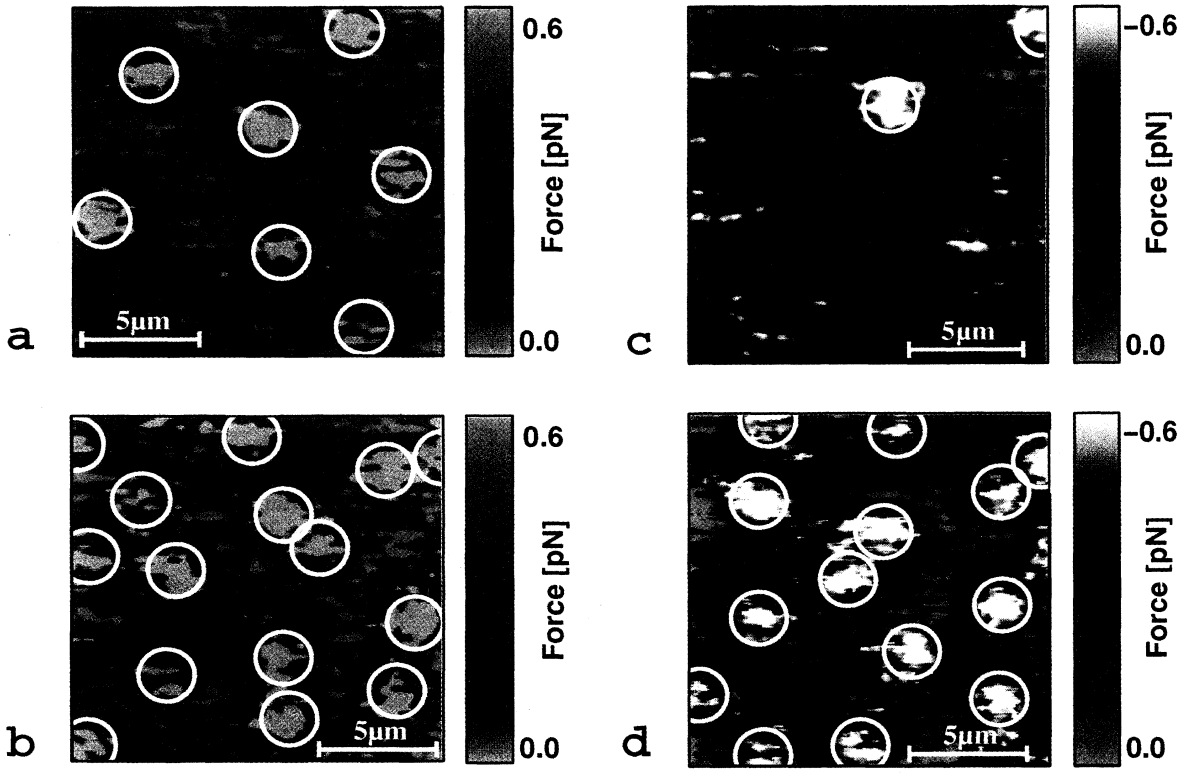

FIG. 2. A specific number of vortices are produced by cooling the sample in different fields: (a) Field 0.093 mT, 7 vortices generating an attractive force; (b) field 0.174 mT, 15 vortices generating an attractive force; (c) field −0.068 mT, 2 vortices generating a repulsive force; (d) field −0.149 mT, 14 vortices generating a repulsive force.

the smallest intervortex distance in our experiments is much larger than the effective penetration depth (see below), the average pinning force per vortex is simply $F_P = j\phi_0 d$, where $d = 300$ nm is the thickness of the YBCO film, $\phi_0 = 2.07 \times 10^{-15}$ Wb, and j is the critical current density, estimated to be around 10^{10} Am^{-2}; we find $F_P \simeq 6 \times 10^{-12}$ N. This is about two orders of magnitude larger than the expected lateral force exerted by the tip.

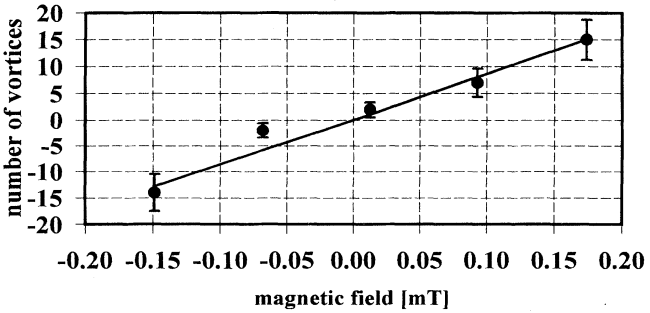

FIG. 3. The number of vortices of Figs. 1(b) and 2(a)–2(d) are plotted versus the applied magnetic field. Negative numbers of vortices are used for vortices producing a repulsive force. The solid line represents a fit to the data which gives a flux of $(1.93 \pm 0.12) \times 10^{-15}$ Wb per single feature. We conclude that these features are images of single vortices carrying one single flux quantum of 2.07×10^{-15} Wb.

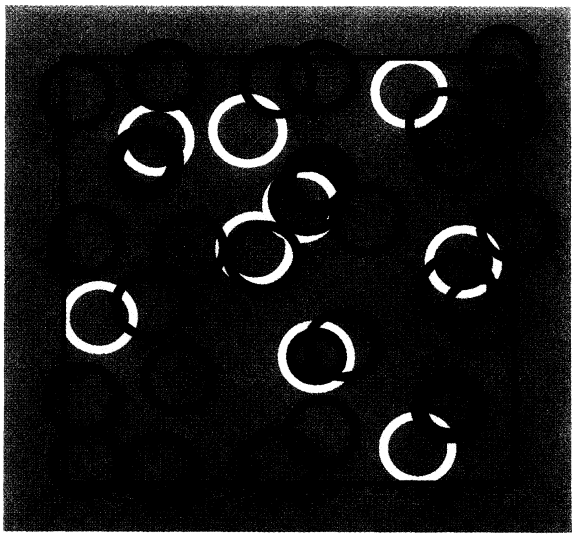

FIG. 4. The figure shows all positions which were occupied by a vortex in the data presented in Fig. 1(b) (white circles), Fig. 2(a) (yellow circles), Fig. 2(b) (red circles), Fig. 2(c) (blue circles), and Fig. 2(d) (black circles). In the 11.6 μm × 14.4 μm sized area, many equivalent pinning centers seem to exist. Note that certain pinning centers are occupied by vortices in at least two images (concentrical circles).

To extract the magnetic radius of the vortices, we fitted a two-dimensional Gaussian function to our data. In the case of attractive vortices, we find a radius (defined to be the distance between the center of the vortex and the point where the force has dropped to e^{-1} of the maximum value) to be between 830 ± 0.2 and 1170 ± 0.4 nm. In the case of repulsive vortices we find a radius between 420 ± 0.2 and 540 ± 0.6 nm. Using the two fluid model

$$\lambda(T) = \lambda(0) \frac{1}{\sqrt{1 - (T/T_c)^4}}$$

and $\lambda_{ab}(0) = 140$ nm, we find $\lambda_{ab}(77\ \mathrm{K}) = 196$ nm. For our thin film with a thickness of $d \sim \lambda$ using

$$\lambda_{ab,\mathrm{eff}}(77\ \mathrm{K}) = \lambda_{ab}(77\ \mathrm{K}) \coth(d/2\lambda),$$

we find for $\lambda_{ab,\mathrm{eff}}(77\ \mathrm{K}) = 305$ nm. Using our model [17] we estimate the force trace above a single vortex and find the radius to be about 600 nm. The calculated value lies between the experimental ones for attractive and repulsive vortices. The difference can be attributed to the influence of the scanning tip.

In summary, we have demonstrated that the MFM is able to image single vortices in the YBCO thin film. We observe a disordered arrangement of vortices. All vortices present in the sample are imaged, and no additional vortices are created and none are dragged along by the tip. Thus the vortices are well pinned over hours at 77 K. The stability of the vortex arrangements suggests that the observed phase is a true superconductor. We thus have established a new experimental method to study directly the reaction of vortices to external disturbances such as temperature, magnetic field, and transport current. The maximum time scale is given by the acquisition time of one image, which is of the order of 1 min. Furthermore, the possibility to correlate the topography to the magnetic field map will give new insights into the nature of the pinning sites, e.g., the role of screw dislocations [31].

We would like to thank T. A. Jung who was involved at the beginning of this project. This work was supported by Swiss National Science Foundation, by the NPF 30, as well as by the Kommission zur Förderung der wissenschaftlichen Forschung. This work has been carried out under a joint study agreement of P. Chaudhari from IBM Watson Research Center and the Institute of Physics, University of Basel.

[1] G. J. Dolan, G. V. Chandrashekhar, T. R. Dinger, C. Feild, and F. Holtzberg, Phys. Rev. Lett. **62**, 827 (1989).
[2] P. Gammel, L. Schneemeyer, J. Waszczak, and D. Bishop, Phys. Rev. Lett. **61**, 1666 (1988).
[3] D. E. Farrel, J. P. Rice, and D. M. Ginsberg, Phys. Rev. Lett. **67**, 1165 (1991).
[4] R. H. Koch, V. Foglietti, W. J. Gallagher, G. Koren, A. Gupta, and M. P. A. Fisher, Phys. Rev. Lett. **63**, 1511 (1989).
[5] P. L. Gammel, L. F. Schneemeyer, and D. J. Bishop, Phys. Rev. Lett. **66**, 953 (1991).
[6] A. Schilling, H. R. Ott, and Th. Wolf, Phys. Rev. B **46**, 14253 (1992).
[7] E. M. Forgan, D. McK. Paul, H. A. Mook, P. A. Timmins, H. Keller, S. Sutton, and J. S. Abell, Nature (London) **343**, 735 (1990).
[8] G. Blatter and B. Ivlev, Phys. Rev. Lett. **63**, 2621 (1993).
[9] H. F. Hess, R. B. Robinson, R. C. Dynes, J. M. Valles, and J. V. Waszczak, Phys. Rev. Lett. **62**, 214 (1989).
[10] H. F. Hess, R. B. Robinson, R. C. Dynes, J. M. Valles, and J. V. Waszczak, J. Vac. Sci. Technol. A **8**, 450 (1990).
[11] R. Berthe, Ph.D. thesis, Universität Giessen/KFA-Jülich, 1991.
[12] H. F. Hess, C. A. Murray, and J. V. Waszczak, Phys. Rev. Lett. **69**, 2138 (1992).
[13] S. Behler, S. H. Pan, P. Jess, A. Baratoff, H.-J. Güntherodt, F. Levy, G. Wirth, and J. Wiesener, Phys. Rev. Lett. **72**, 1750 (1994).
[14] Ch. Renner, A. D. Kent, Ph. Niedermann, O. Fischer, and F. Levy, Phys. Rev. Lett. **67**, 1650 (1991).
[15] C. Renner, Ph.D thesis, University of Geneva, 1993.
[16] H. Hug, T. Jung, H.-J. Güntherodt, and H. Thomas, Physica C **175**, 357 (1991).
[17] A. Wadas, O. Fritz, H. J. Hug, and H.-J. Güntherodt, Z. Phys. B **88**, 317 (1992).
[18] O. Fritz, M. Wülfert, A. Wadas, H. J. Hug, H.-J. Güntherodt, and H. Thomas, Phys. Rev. B **47**, 384 (1993).
[19] K. Haralda, T. Matsuda, H. Kasai, J. E. Bonevich, T. Yoshida, U. Kawabe, and A. Tonomura, Phys. Rev. Lett. **71**, 3371 (1993).
[20] A. M. Chang *et al.*, Europhys. Lett. **20**, 645 (1992).
[21] P. Rice and J. Moreland, IEEE Trans. Magn. **27**, No. 6 (1991).
[22] A. Moser, H. J. Hug, Th Jung, U. D. Schwarz, and H.-J. Güntherodt, Meas. Sci. Technol. **4**, 769 (1993).
[23] H. J. Hug, A. Moser, Th. Jung, A. Wadas, I. Parashikov, and H.-J. Güntherodt, Rev. Sci. Instrum. **64**, 2920 (1993).
[24] T. R. Albrecht, P. Grütter, D. Rugar, and D. P. E. Smith, Ultramicroscopy **42–44**, 1638 (1992).
[25] H. J. Hug, A. Moser, O. Fritz, I. Parashikov, H.-J. Güntherodt, and Th. Wolf, Physica B **194–196**, 377 (1994).
[26] A. Moser, H. J. Hug, O. Fritz, I. Parashikov, and H.-J. Güntherodt, J. Vac. Sci. Technol. B **12**, 1586 (1994).
[27] H. J. Reittu and R. Laiho, Supercond. Sci. Technol. **5**, 448 (1992).
[28] A. Wadas, H. J. Hug, and H.-J. Güntherodt, J. Appl. Phys. **72**, 203 (1992).
[29] M. P. A. Fisher, Phys. Rev. Lett. **62**, 1414 (1989); D. A. Fisher, M. P. A. Fisher, and D. A. Huse, Phys. Rev. B **43**, 130 (1991).
[30] D. R. Nelson and V. M. Vinokur, Phys. Rev. Lett. **68**, 2398 (1992); Phys. Rev. B **48**, 13060 (1993).
[31] J. Mannhart, D. Anselmetti, J. G. Bednorz, A. Catana, Ch. Gerber, K. A. Müller, and D. G. Schlom, Z. Phys. B **86**, 177 (1992).

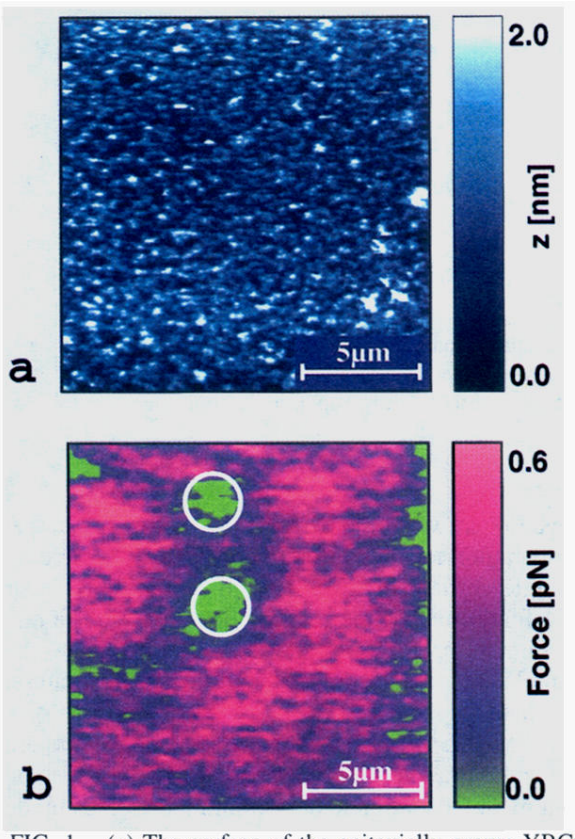

FIG. 1. (a) The surface of the epitaxially grown YBCO films is extremely smooth. The small hills have a diameter of about 50 nm and a height of only a few nanometers. These hills are believed to be screw dislocations. The step structure cannot be resolved, since the radius of the tip is expected to be around 30 nm. This topographical image is acquired with the tip in contact with the surface of the sample. (b) The same area is imaged with the tip not in contact with the sample. The two, circular features produce an attractive force of only 6×10^{-13} N. These features are images of single vortices. The sample was cooled in a field of 0.013 mT.

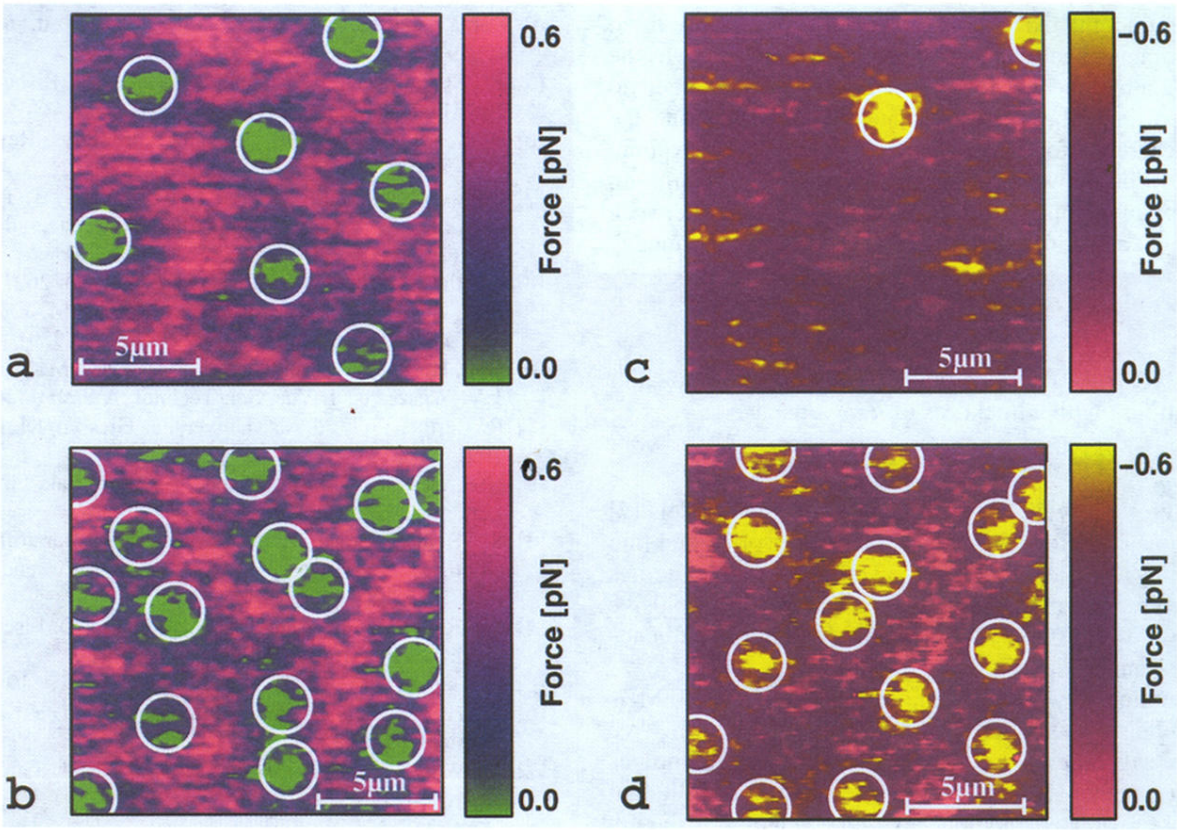

FIG. 2. A specific number of vortices are produced by cooling the sample in different fields: (a) Field 0.093 mT, 7 vortices generating an attractive force; (b) field 0.174 mT, 15 vortices generating an attractive force; (c) field −0.068 mT, 2 vortices generating a repulsive force; (d) field −0.149 mT, 14 vortices generating a repulsive force.

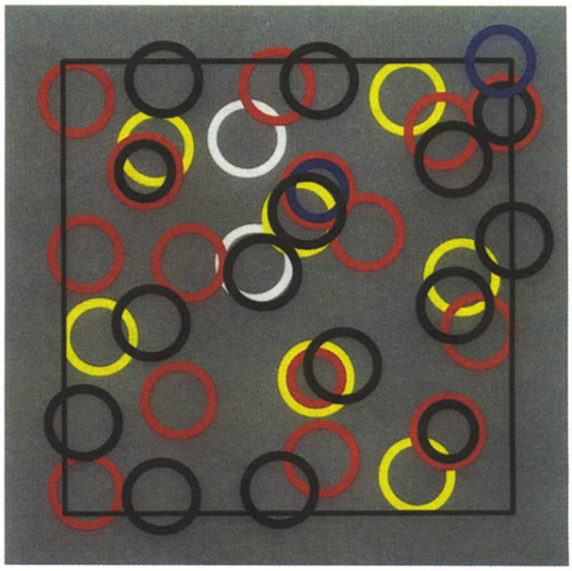

FIG. 4. The figure shows all positions which were occupied by a vortex in the data presented in Fig. 1(b) (white circles), Fig. 2(a) (yellow circles), Fig. 2(b) (red circles), Fig. 2(c) (blue circles), and Fig. 2(d) (black circles). In the 11.6 μm $\times$ 14.4 μm sized area, many equivalent pinning centers seem to exist. Note that certain pinning centers are occupied by vortices in at least two images (concentrical circles).